Quantitative diffusion tensor imaging in cerebral palsy due to periventricular white matter injury

Bejoy Thomas,[1,4,*] Maria Eyssen,[2,*] Ronald Peeters,[1] Guy Molenaers,[3] Paul Van Hecke,[1] Paul De Cock[2] and Stefan Sunaert[1]

[1]Department of Radiology, [2]Department of Pediatrics, and [3]Department of Orthopedics, University Hospitals, KUL, Leuven, Belgium and [4]Department of Radiology, Sree Chitra Tirunal Institute for Medical Sciences and Technology, Trivandrum, Kerala, India

Correspondence to: Stefan Sunaert, Department of Radiology, University Hospitals, Katholieke Universiteit Leuven, Herestraat 49, 3000 Leuven, Belgium
E-mail: stefan.sunaert@uz.kuleuven.be
*These authors contributed equally to this work

Periventricular white matter injury (PWI) is a major form of brain injury observed in congenital hemiparesis. The aim of this study is to determine the usefulness of diffusion tensor imaging (DTI) and fibre tracking in delineating the primary and secondary degenerative changes in cerebral white matter and deep grey matter in patients with spastic cerebral palsy due to PWI and to look for any possible reorganization of the axonal architecture. Five hemiparetic cerebral palsy patients (median age 14 years) with known PWI were prospectively studied with DTI of the brain at 1.5T and quantitatively compared with five age and sex matched controls. Fibre tracts for various corticofugal, thalamocortical and association tracts were generated and analysed for the DTI fibre count and for diffusion parameters. A region of interest based analysis was performed for the directionally averaged mean diffusivity (D_{av}) and fractional anisotropy (FA) values in various white matter locations in the brain and the brainstem and in the deep grey matter nuclei. Group statistics were performed for these parameters using Mann–Whitney U-test comparing the affected sides in patients with either side in controls and the unaffected side in hemiparetics. There was significant reduction in DTI fibre count on the lesional side involving corticospinal tract (CST), corticobulbar tract (CBT) and superior thalamic radiation in the patient group compared with controls. Also there was an increase in DTI fibre count in the unaffected side of the hemiparetic patients in CST and CBT, which reached statistical significance only in CBT. The corpus callosum, cingulum, superior longitudinal fasciculus and middle cerebellar peduncle failed to show any significant change. ROI measurements on the primary site of white matter lesion and the thalamus revealed a significant increase in D_{av} and decrease in FA, suggesting primary degeneration. The CST in the brainstem, the body of corpus callosum and the head of caudate and lentiform nuclei showed features of secondary degeneration on the affected side. The CST on the unaffected side of hemiparetics was found to have a significant decrease in D_{av} and an increase in FA. Thus the degeneration of various motor and sensory pathways, as well as deep grey matter structures, appears to be important in determining the pathophysiological mechanisms in patients with congenital PWI. Also evidence suggesting the reorganization of sensorimotor tracts in the unaffected side of spastic hemiparetic patients was noted.

Introduction

Congenital hemiplegia due to prenatal or perinatal brain damage has become the most common form of cerebral palsy among children born at term, and second to diplegia among children born prematurely (Hagberg et al., 2001). Periventricular leukomalacia (PVL) is a major form of brain injury observed in survivors of premature birth. Occasionally, it is found after uneventful pregnancy and birth, probably due to intra-uterine brain damage without obvious aetiology (Kwong et al., 2004). When confined to one side, hemiplegia can be found as the corresponding clinical picture; but bilateral signs of brain lesion giving rise to unilateral motor involvement have been described as well (Niemann, 2000). Hypoxic-ischaemic or inflammatory insult to the developing brain during the early third trimester of intrauterine life is generally believed to be the key aetiological factor in this form of cerebral palsy (Johnston et al., 2001a; Volpe, 2001; Payam and Andrew, 2002). Another form of periventricular white matter injury (PWI) consists of unilateral periventricular venous infarction (PVI), generally as a consequence of haemodynamic changes associated with intraventricular haemorrhage, and it can be found in preterms as well as in full-term born hemiplegics (de Vries et al., 2001; Takanashi et al., 2003). It is not always possible to distinguish between these two forms of PWI (de Vries et al., 2001).

Structural MRI features in this condition (periventricular T2 hyperintensity; white matter volume loss and ventricular dilatation) and their clinical correlates are well described (Cioni et al., 1992; Schouman-Claeys et al., 1993; Melhem et al., 2000; Hashimoto et al., 2001; Marti-Bonmati et al., 2001). However, marked overlap of imaging features has been observed in individual cases. It is generally assumed that the damage to the corticospinal (pyramidal) tract accounts for most motor deficits as originally proposed by Banker and Larroche (1962). Meanwhile the exact correlation between brain damage and motor impairment still remains unclear, one recent report suggesting the role of involvement of sensory pathways (Hoon et al., 2002).

Conventional MRI cannot delineate the white matter pathways of human brain precisely and hence is of little use in differentiating the individual tracts involved in this condition either primarily or secondarily due to maldevelopment and/or degeneration.

Diffusion tensor imaging (DTI) is a modification of the MRI technique that is sensitive to the Brownian motion of water molecules in biological tissues (Le Bihan and Basser, 1995; Basser and Pierpaoli, 1996) and is a new clinical method that can demonstrate the orientation and integrity of white matter fibres in vivo (Wakana et al., 2004). Within cerebral white matter water molecules diffuse more freely along the direction of axonal fascicles than across them, arising from the restriction of free water diffusion by the axonal membrane, axonal microtubuli and the axonal myelin sheath (Le Bihan et al., 1986; Moseley et al., 1990; Pierpaoli et al., 1996). Such directional dependence of diffusivity is termed anisotropy. An integrated MR measure of water diffusion in at least six non-collinear directions is used to calculate the diffusion tensor (D), from which fractional anisotropy (FA—the amount of anisotropy) and the directionally averaged mean diffusivity (D_{av}) can be derived (Basser and Pierpaoli, 1998). By combining anisotropy data with the directionality it is possible to obtain estimates of fibre orientation. This has led to fibre tractography (FT) in which 3D pathways of white matter tracts are reconstructed by sequentially piecing together discrete and shortly spaced estimates of fibre orientation to form continuous trajectories (Mori et al., 1999, 2002; Basser et al., 2000).

In the present study, we used DTI-based colour orientation maps and FT in five children with cerebral palsy and an MRI proven structural periventricular lesion, for the quantitative evaluation of various white matter pathways in an attempt to unravel the structural brain damage underlying motor disability. Different projection and association tracts were developed bilaterally and were statistically compared with those of five (age and sex matched) normal children in terms of DTI fibre count, D_{av} and FA values. We hypothesized that the corticofugal and thalamocortical projection fibres might show significant diffusion parameter changes on the affected side.

In addition, a region of interest (ROI) based analysis was performed with D_{av} and FA values calculated in various regions of the cerebral white matter, deep grey matter and brainstem in order to determine the diffusion tensor signatures of primary and secondary degenerative changes in this condition. White matter tracts, especially the corticospinal tract (CST) and the corticobulbar tract (CBT) were studied in detail bilaterally, for possible reorganization. The CST was also studied at the upper pons level with cross-sectional area ratio measurements to confirm Wallerian degeneration.

Methods

We recruited prospectively five cerebral palsy patients (12–16 years, median age 14 years, 3M, 2F) from the Child Neurology Clinic of the University Hospitals Leuven with known PWI and structural changes detected on conventional MRI; as well as five age and sex matched normal children who served as controls. Our institutional ethical committee approved the study and informed written consent was obtained from all the participants and their parents.

Inclusion criteria for the patient group were spastic hemiparesis, with or without clinical sensory involvement, no documented cognitive or intellectual impairment and MRI documented unilateral PWI. Minimal hyperintensive changes in the periventricular white matter of the hemisphere contralateral to the lesion, as described by many authors in hemiparetic affected children, were accepted (Niemann, 2000). The Gross Motor Function Classification System (GMFCS) was used for the clinical grading of severity of motor disability (Palisano et al., 1997), and all our patients were classified as level 1 (mildest level) (Table 1). The controls were neurologically normal children scanned as part of another larger functional neurophysiology study. All the control subjects were right-handed. In the patient group, the hemiparetics were oriented to use the contralateral normal hand. All the subjects underwent a thorough, video recorded,

Table 1 Demographic, clinical and conventional MRI data

Patient	Age	Sex	Birth weight (kg)	Pre and perinatal history	Neurological evaluation	MRI	Clinical grade (GMCS)
1	16	F	2.1	Term, CS (FPD)	Left hemiparesis	Right moderate cystic PWI	Level 1(B)
2	12	M	3.1	Term, CS	Right hemiparesis	Left large cystic PWI	Level 1(B)
3	13	M	2.8	Term, forceps	Left hemiparesis	Right mild PWI, small cyst	Level 1(A)
4	16	M	2.8	Term, normal	Left hemiparesis	Right mild PWI, small cyst	Level 1(A)
5	15	F	3.6	Term, normal	Left hemiparesis	Right mild PWI	Level 1(A)

CS, caesarian section; FPD, feto-pelvic disproportion; PWI, periventricular white matter injury; GMFCS, gross motor function classification system (see text); Level 1A, no braces needed; 1B, braces needed.

neurological examination by a paediatric neurologist (M.E.) to confirm the findings in patients and to exclude any deficits in controls.

MR data acquisition

All the patients and controls underwent MR examination on a 1.5 T scanner (Intera, Philips, Best, The Netherlands), without sedation or general anaesthesia. The sequences included a T1 weighted coronal 3D TFE, T2 weighted axial FLAIR and a DTI SE EPI (diffusion weighted, single shot, spin-echo echoplanar imaging), with a data acquisition matrix = 96×96; field of view = 200×200 mm; TR = 1758 ms and TE = 64 ms. Sixty eight contiguous 2 mm thick slices covering the entire brain and the brainstem were acquired in axial direction, parallel to AC-PC line. Bi-lobed diffusion gradients were applied along 15 non-collinear directions with a *b* value of 900 s/mm^2. In addition a, *b*0 image was also obtained. For the DTI, three signal averages with SENSE factor 2 were used with a resultant scan time of 15.2 min.

Post-processing of MR data

The DTI and 3D TFE datasets were transferred to a workstation (Pride, Philips, Best, The Netherlands). All the images were at first visually inspected for apparent artefacts. The DTI images were then processed and coregistered to remove image distortion that arises from the effect of eddy currents on the EPI readout. The diffusion tensor dataset for each voxel was generated including eigenvalues and eigenvectors using multivariate fitting. DEC (diffusion encoded), FA-weighted images were calculated according to the scheme proposed by Pajevic and Pierpaoli (1999). Then DTI-based colour maps were generated. The eigenvector associated with the largest eigenvalue along *x* direction was assigned to red (left–right); along *y*, green (anterior–posterior) and along *z*, blue (superior–inferior). Intensities of maps were scaled in proportion to FA. These images were then coregistered with the axially reformatted 3D TFE volume using SPM2 (Statistical Parametric Mapping, Wellcome Department of Imaging Neuroscience, University College London).

Three-dimensional tract reconstruction

Tract reconstruction was performed by fibre assignment by continuous tracking (FACT) method (Le Bihan and Basser, 1995; Basser and Pierpaoli, 1996; Basser and Pierpaoli, 1998). In this technique, the eigenvector associated with the largest eigenvalue is used as an indicator of fibre orientation. The CST, CBT, thalamocortical connections (anterior, superior and posterior thalamic radiations—ATR, STR and PTR, respectively), cingulate fasciculus (CG), and the superior longitudinal fasciculus (SLF) were developed bilaterally both in patients and volunteers (Makris *et al.*, 1997). In addition total corpus callosum (CC) and middle cerebellar peduncle (MCP) fibres were also generated. They were produced by tracking through two

ROIs and an 'AND' operation using 'brute force' approach, by modification of the method described previously (Mori *et al.*, 2002; Wakana *et al.*, 2004). Two neuroradiologists (S.S. and B.T.) separately marked all the ROI on tensor colour maps and on the coregistered anatomy images, and performed the measurements of DTI fibre count, FA and D_{av} independently. The values of DTI fibre count, FA and D_{av} agreed well (κ-test > 0.6) for the two observers, and therefore the reported values are the mean of the two observers.

Quantitative analysis

A DTI fibre count was performed for each of the tracts generated in all subjects. In addition D_{av} and FA values along the tracts were studied for CST, CBT, STR and CC.

DTI fibre count represents the number of streamlines composing a particular tract. The relationship between this number of streamlines and the real number of axons has not yet been described completely, and is highly dependent on the resolution of the DTI scan (2 mm isotropic in this study), and on the chosen FA and angular deflection thresholds chosen in the FACT algorithm. Slightly different FA and angular deflection thresholds were used in order to minimize erroneous branching and/or contribution of fibres not belonging to the particular tract under study. These thresholds were derived from pilot studies with healthy adult or adolescent volunteers, and ranged between 0.20 and 0.25 for FA threshold, and between 0.75 and 0.85 for the angular deflection threshold. These thresholds are in good agreement with thresholds used in other DTI studies (Mori *et al.*, 2002; Wakana *et al.*, 2004). The positions of different ROI, the FA and angular deflection thresholds used in generating the different tracts are summarized in Fig. 1. Great care was taken to standardize the position and size of the ROIs across subjects and this was performed in accordance with the methods of Mori *et al.*, 2002 and Wakana *et al.*, 2004. For a particular pathway the same settings were used in all the patients and volunteers, and no changes were introduced for the different age of the children. Therefore DTI fibre count of a given tract can be compared quantitatively between these subjects under study.

ROI analysis

Bilaterally symmetrical ROI measurements for D_{av} and FA were performed separately at the primary site of insult (periventricular region), the CST in brainstem (at three levels: upper medulla, upper and lower pons) and the deep grey matter (thalamus, head of the caudate and the lentiform nucleus). The CC was also studied at three levels (genu with rostrum, body and splenium) on the mid-sagittal image. The locations of the ROI used are detailed in Fig. 2A. For the ROI of the primary site of insult, a manual delineation of the T2 hyperintense lesion was performed, and the contralateral ROI in normal appearing white matter was obtained through symmetric
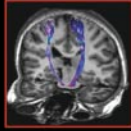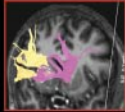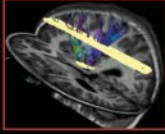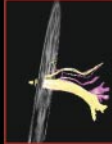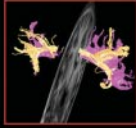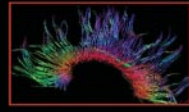
Fig. 1 ROI and threshold settings in different fibre tracts. The representative images of various fibre tracts studied, with the locations of ROI marked and the FA and angular deflection thresholds used in generating them are demonstrated. Same thresholds were used for a particular tract in all the subjects, and hence intersubject comparison was possible for any particular tract. ROI = regions of interest, FA = fractional anisotropy, CST = corticospinal tract, CBT = corticobulbar tract, ATR = anterior thalamic radiation, STR = superior thalamic radiation, PTR = posterior thalamic radiation, CG = cingulate fasciculus, SLF = superior longitudinal fasciculus, MCP = middle cerebellar peduncle and CC = corpus callosum, Rt = right, Lt = left.

mirroring. For the healthy volunteers, the control ROI for the primary insult was a ROI positioned and sized according to the averaged positions and sizes of the lesions in the patients. Other ROIs were placed according to the anatomical delineation of the structure of interest, and were not always symmetrical. Also the brainstem ROIs in patients with unilateral PWI were asymmetric in size, in an attempt to include only the CST area (blue) on the colour map.

In addition, the exact cross-sectional area of the CST at the level of the upper pons was measured in each of the patients and the volunteers on the DTI colour maps and were superimposed on the corresponding coregistered axial anatomical slices. A ratio of the area of CST on either side, to the total cross-sectional area of the upper pons, was also calculated (Fig. 2B).

Statistical analysis

The data on the affected side in the hemiparetic patients were compared with those on the normal side and with those of the controls in all the patients using Mann–Whitney *U*-test. This test was chosen because the sample size was relatively small and some diffusion parameters under investigation, like FA, have a non-Gaussian distribution (Pierpaoli *et al.*, 1996; Pajevic and Pierpaoli, 1999). Group comparison for 10 datasets on controls, five datasets on affected side and five sets on unaffected side of the patients were performed for each of the fibre tracts and the ROI. The threshold for statistical significance was set at $P = 0.05$. In addition a right side versus left side comparison was done in control subjects to search for any possible significant variability in fibre statistics.

Results
Patient history and conventional MRI findings

The demographic, clinical and conventional MRI findings are summarized in Table 1. All the control subjects were assessed to be neurologically normal.

The five patients had spastic hemiparesis involving limbs contralateral to the side of the detected lesion on conventional MRI. Patient 1 was born, after an uneventful pregnancy, by
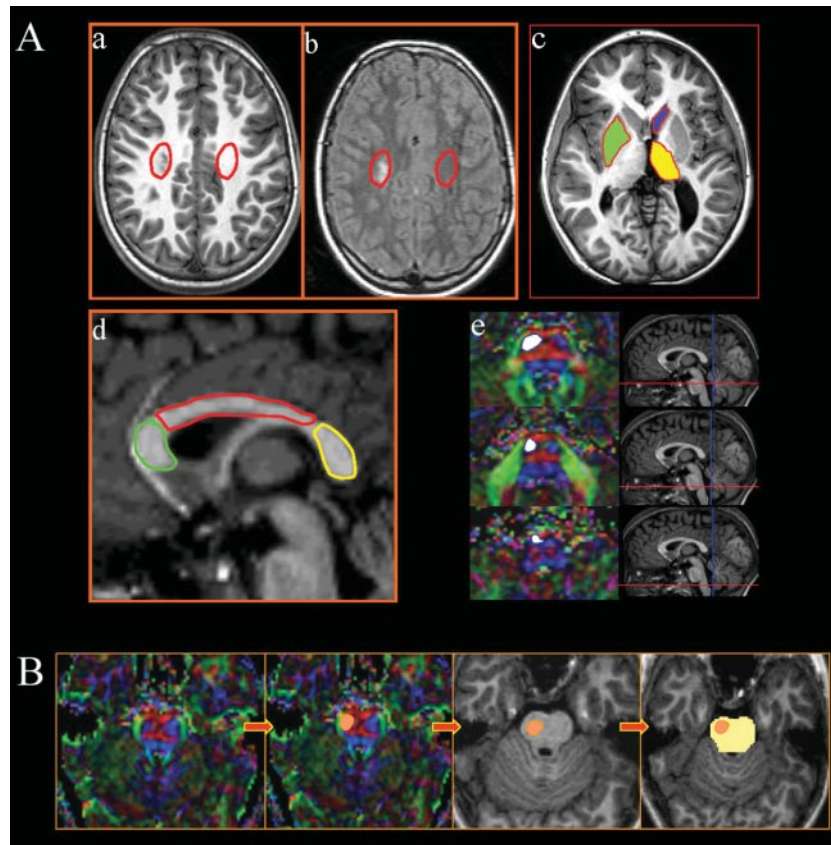
Fig. 2 (**A**) ROI analysis of diffusion parameters. The locations of the ROI marked for the analysis of various diffusion parameters (see text), are shown at the sites of primary periventricular lesion (red) (a and b), deep grey matter nuclei (yellow, green, blue) (c), the different regions of the corpus callosum (green, red, yellow) (d) and the pyramidal tract in the brainstem at different levels (white) (e) (note the corresponding sagittal reference images). All the sites were studied bilaterally except the corpus callosum. The ROI were placed on the coregistered anatomy sections in the case of primary sites, deep grey matter and the corpus callosum and on the colour maps for the CST in the brainstem. Note also that the corresponding axial FLAIR image (b) was used for better delineation of the primary site in subtle lesions. (**B**) Cross-sectional area ratio measurements of pyramidal tract in upper pons. The cross-sectional area of the pyramidal tract in the upper pons was marked at first on the axial colour map and then superimposed on the corresponding anatomy sections (orange). The total cross-sectional area of the pons at this level was also measured (yellow) and a ratio was calculated. This was repeated for the contralateral pyramidal tract.

Caesarean section performed at term because of the presumption of fetopelvic disproportion. However, the birth weight was only 2.1 kg (below third percentile, dysmaturity), so the intra-uterine period might have been compromised despite the history of normal pregnancy. In patient 2, the only event was an episode of maternal syncope, probably hypoglycaemic (not documented) towards the end of the third trimester; the child was born by (repeat) Caesarean section. At 6 months pregnancy, the mother of patient 3 underwent a partial CO-intoxication, without loss of consciousness. The child was born at term with forceps but without further complications. The prenatal and perinatal history was completely uneventful in patient 4, as well as in patient 5.

In all children, the parents noticed asymmetrical movements before or around the age of 1 year. First imaging studies confirming the underlying brain damage were done subsequently.

Visual inspection of the 3D TFE and the FLAIR images of this study (Fig. 3) confirmed the previously detected findings in all the patients. The lesions varied in severity from mild hyperintensity detected in the periventricular region on FLAIR images to large cystic areas with resultant white matter loss and dilatation of the ipsilateral lateral ventricle. Although patients 1 and 2 might show PVI rather than PVL, in our opinion, it was not possible in the other patients to distinguish with certainty between those two forms of PWI. It should be noted that clinically all patients were clearly hemiparetic. However, this does not exclude minimal hyperintense changes in periventricular white matter in patients 2, 4 and 5, as described by many authors in hemiparetic affected children (Niemann, 2000).

Analysis of the fibre tracts

Table 2 details the mean DTI fibre count, FA and D_{av} values in different fibre tracts studied in patient and control groups, and Table 3 shows the statistical significance (*P*- value) for group comparison of these parameters between controls (on both the sides) and patients (on the affected and
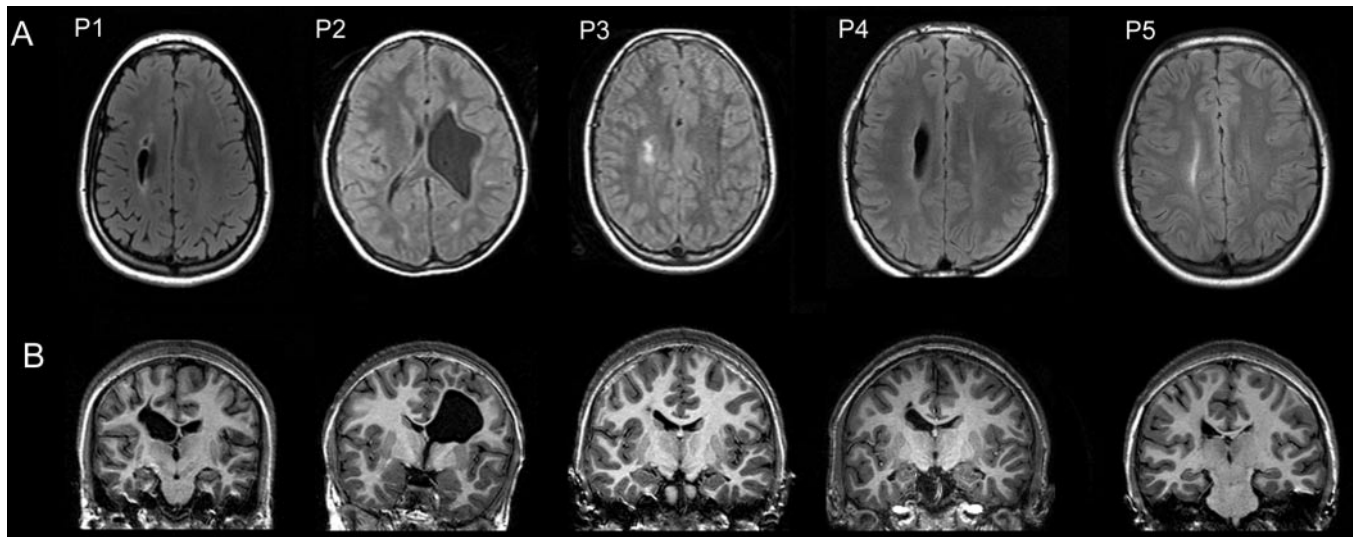
Fig. 3 Axial and coronal MRI in patients. The representative axial images on FLAIR (**A**) and coronal images on T1 (**B**) are shown.

Table 2 Mean DTI fibre count, D_{av} and FA values in control and patient groups

Tract	Controls			Patients unaffected side			Patients affected side		
	DTI fibre count	FA	D_{av}	DTI fibre count	FA	D_{av}	DTI fibre count	FA	D_{av}
CST									
R	2516	0.59	0.79	2956	0.57	0.82	40	0.52	0.83
L	2774	0.59	0.78						
CBT									
R	1170	0.51	0.81	1690	0.51	0.84	689	0.47	0.89
L	1131	0.52	0.81						
ATR									
R	3252	0.40	0.82	2059	0.42	0.79	1787	0.40	0.81
L	3711	0.41	0.79						
STR									
R	222	0.45	0.76	186	0.45	0.77	90	0.45	0.85
L	159	0.46	0.76						
PTR									
R	194	0.43	0.83	83	0.48	0.83	371	0.46	0.87
L	1372	0.50	0.79	1032	0.46	0.86	20	0.48	0.88
CG									
R	4641	0.46	0.80	2700	0.46	0.80	2215	0.42	0.87
L	3530	0.49	0.79						
SLF									
R	1206	0.46	0.79	1342	0.45	0.79	824	0.44	0.82
L	1003	0.47	0.79						
MCP	4798	0.49	0.81	–	–	–	3684	0.48	0.76
CC	6838	0.54	0.82	–	–	–	5442	0.51	0.88

R, right; L, left; CST, corticospinal tract; CBT, corticobulbar tract; ATR, anterior thalamic radiation; STR, superior thalamic radiation; PTR, posterior thalamic radiation; CG, cingulum; SLF, superior longitudinal fasciculus; MCP, middle cerebellar peduncle; CC, corpus callosum; FA, fractional anisotropy; D_{av}, directionally averaged mean diffusivity (Trace D/3).

unaffected sides). Figs 4–6 summarize these changes in the most important tracts.

Changes in the affected hemisphere of PWI children

When comparing normal controls with PWI patients, a significant reduction in DTI fibre count on the side ipsilateral to the periventricular lesion was observed in the CST (mean DTI fibre count of normal controls = 2645, mean DTI fibre count of PWI patients = 40, $P = 0.0007$), CBT (mean DTI fibre count of normal controls = 1151, mean DTI fibre count of PWI patients = 689, $P = 0.0400$), and STR (mean DTI fibre-count of normal controls = 191, mean DTI fibre count of PWI patients = 90, $P = 0.0400$). Similarly, when comparing the unaffected hemisphere with the affected side in the patients,

Table 3 Statistical significance of comparison between controls and patients: *P*-values

Tract	PT versus control affected side			PT versus control unaffected side			PT affected versus unaffected side			Contol RT versus LT side		
	n	FA	D_{av}	*n*	FA	D_{av}	*n*	FA	D_{av}	*n*	FA	D_{av}
CST	**0.0007**	**0.0007**	**0.0080**	0.3710	0.1292	0.3097	**0.0079**	0.0556	0.6905	0.6905	0.8413	0.5476
CBT	**0.0400**	**0.0013**	**0.0013**	**0.0127**	0.9530	0.1645	**0.0159**	**0.0317**	0.0952	0.5476	0.6905	0.8413
ATR	0.2065			0.1645			0.8413			1.0000		
STR	**0.0400**	0.5135	**0.0027**	0.9530	0.4396	1.000	**0.0317**	0.6905	**0.0079**	0.4206	1.000	1.000
PTR	0.3097			0.7679			0.1508			**0.0079**		
CG	0.4396			0.7679			0.8413			0.4206		
SLF	0.4396			0.7679			0.2222			0.8413		
MCP	0.5556			–			–			–		
CC	0.2857	0.2857	0.0635	–			–			–		

Mann–Whitney *U* test was used for all comparisons, the statistical significance level was set at *P* = 0.05. Significant ones are marked in bold. PT, patients; RT, right; LT, left; CST, corticospinal tract; CBT, corticobulbar tract; ATR, anterior thalamic radiation; STR, superior thalamic radiation; PTR, posterior thalamic radiation; CG, cingulum; SLF, superior longitudinal fasciculus; MCP, middle cerebellar peduncle; CC, corpus callosum; *n*, DTI fibre count; FA, fractional anisotropy; D_{av}, directionally averaged mean diffusivity (Trace D/3).
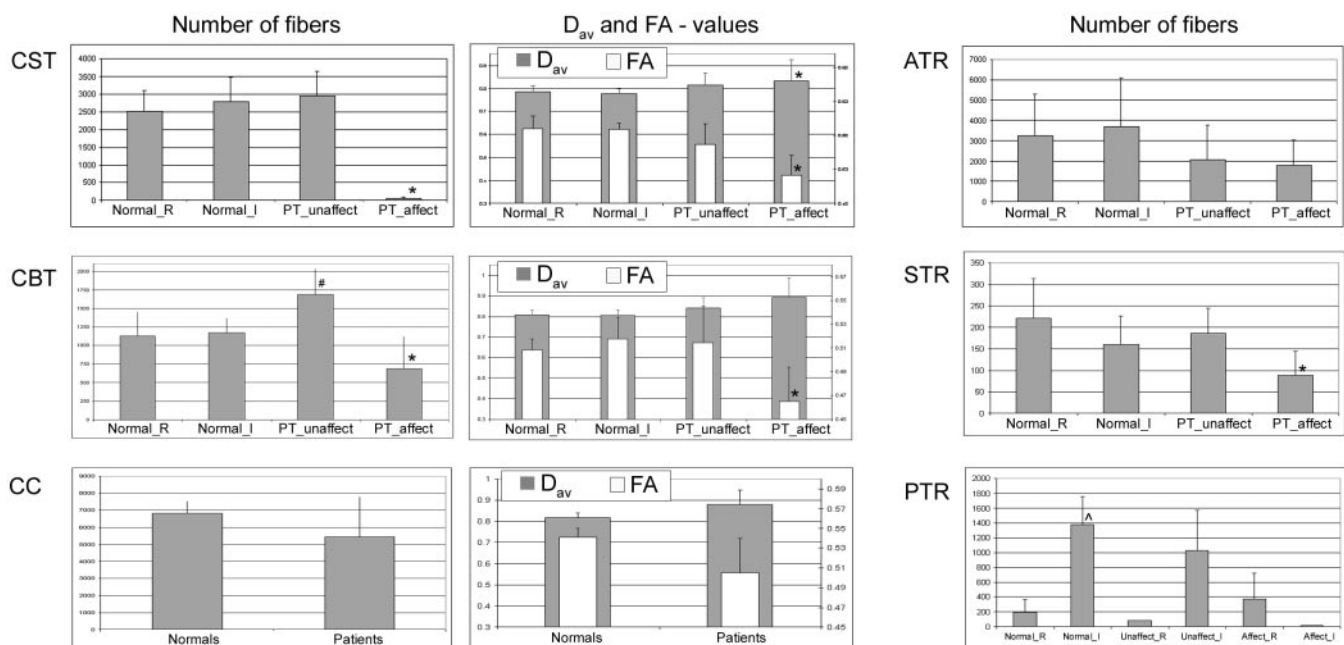

Fig. 4 DTI fibre count, Dav and FA values in different tracts. The distribution of the DTI fibre count, directionally averaged mean diffusivity (Dav) and FA values in the control group and in the affected and unaffected sides of the patients are shown in various important fibre tracts. Note the marked reduction in number of fibres in CST and CBT on the affected side of patients, with a corresponding increase in Dav and a reduction in FA. There is a 'compensatory' increase in number of fibres on the unaffected side in patients. Among the three thalamic radiations studied (ATR, STR, PTR), only STR showed statistically significant reduction in number of fibres on the affected side of patients. PTR demonstrated significant variability in number of fibres between right and left sides of controls. (Error bars indicate SDs, * = statistically significant change on affected side of patients, # = same on unaffected side of patients and ^ = same between the right and left sides in control subjects).

a significant decrease in DTI fibre count was noted in the same CST, CBT and STR. The other studied tracts, notably the ATR, PTR, CG, SLF, MCP and CC, did not show significant differences in DTI fibre count when compared with the controls or unaffected side of the patients (see Figs 7 and 8).

The FA on the affected sides showed a significant decrease within the CST (mean FA of controls = 0.59, mean FA of patients = 0.52, *P* = 0.0007) and CBT (mean FA of controls = 0.515, mean FA of patients = 0.47, *P* = 0.0013) when compared

with the normal controls. The D_{av} showed a significant increase within the CST (mean D_{av} of controls = 0.785, mean D_{av} of patients = 0.83, *P* = 0.0080), CBT (mean D_{av} of controls = 0.81, mean D_{av} of patients = 0.89, *P* = 0.0013) and STR (mean D_{av} of controls = 0.76, mean D_{av} of patients = 0.85, *P* = 0.0027). FA and D_{av} were not significantly different in the ATR, PTR, CG, SLF, MCP and CC when compared with the controls or with the unaffected hemisphere of the patients.
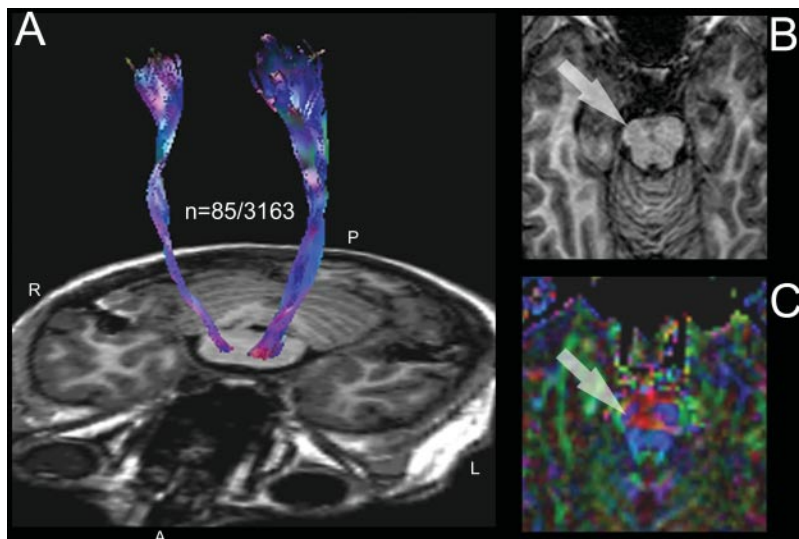
Fig. 5 Corticospinal tract. (**A**) CST in patient 5 shows a significantly reduced number of fibres on the affected right side. (**B**) Axial anatomy section through the midbrain shows atrophy of the right cerebral peduncle (arrow) due to Wallerian degeneration of CST, which is better demonstrated on DTI colour maps. Note the marked rarefaction of the CST (blue) on the affected side (arrow). *n* = DTI fibre count.
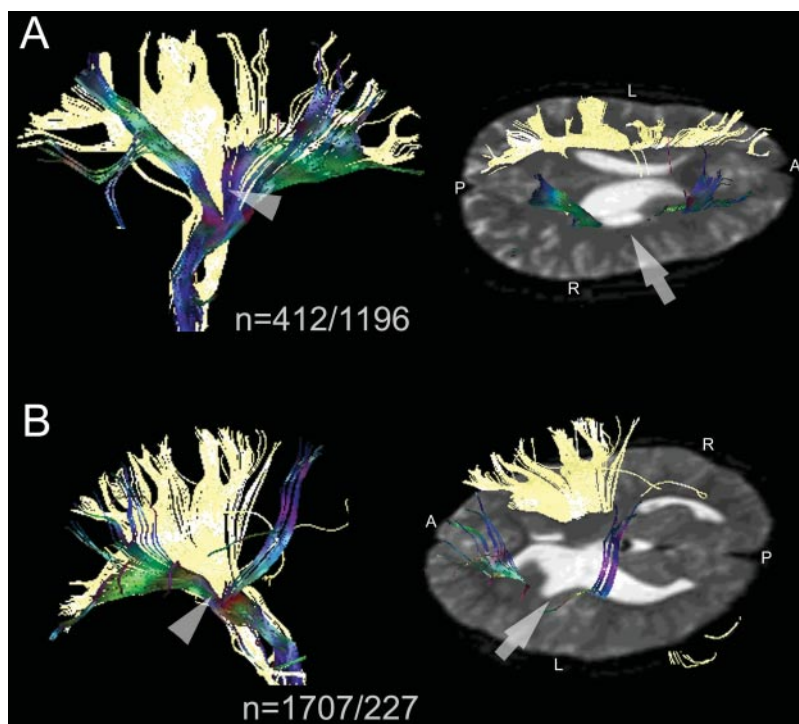

Fig. 6 Corticobulbar tract (**A**) CBT in patient 1 (P1) shows a marked reduction in number of fibres on the affected side (right). (**B**) There is similar change in this tract in P2 on the affected left side. Note also the wedge shaped deficit in CBT on the lesional sides (arrow heads) corresponding to the periventricular lesion (arrow). (*n* = DTI fibre count, colour codes for the fibres, bright yellow = unaffected side, and fractional anisotropy colors = affected side).

Changes in the unaffected hemisphere of PWI children

There was an absolute increase in DTI fibre count on the unaffected side compared with controls in the CBT (mean DTI fibre count of controls = 1151, mean DTI fibre count of patients = 1690, $P = 0.0127$) and a similar trend in the

CST (mean DTI fibre count of controls = 2645, mean DTI of patients = 2956).

Interhemispheric differences in controls

None of the tracts studied in the normal children showed a left–right asymmetry, except for the PTR where significantly
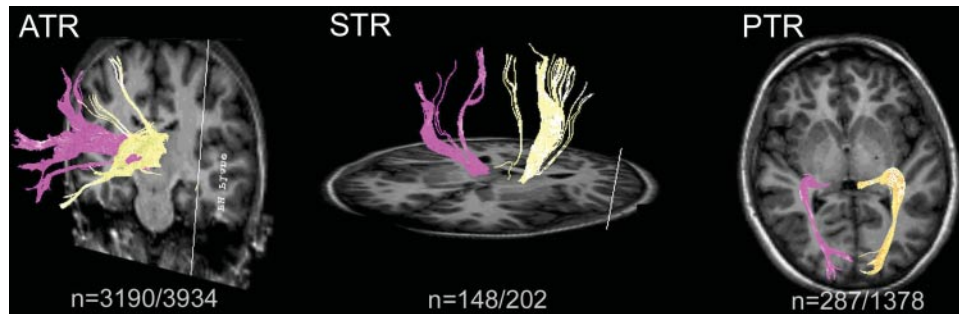
Fig. 7 Thalamic radiations. Representative images of anterior (P5), superior (P3) and posterior (P5), thalamic radiations (ATR, STR and PTR) are shown. Note the significant reduction in fibre number on the affected right side in STR and PTR in these patients. No significant change was noted in the ATR. (*n* = DTI fibre count; colour codes for the fibres, bright yellow = unaffected side, bright pink = affected side).
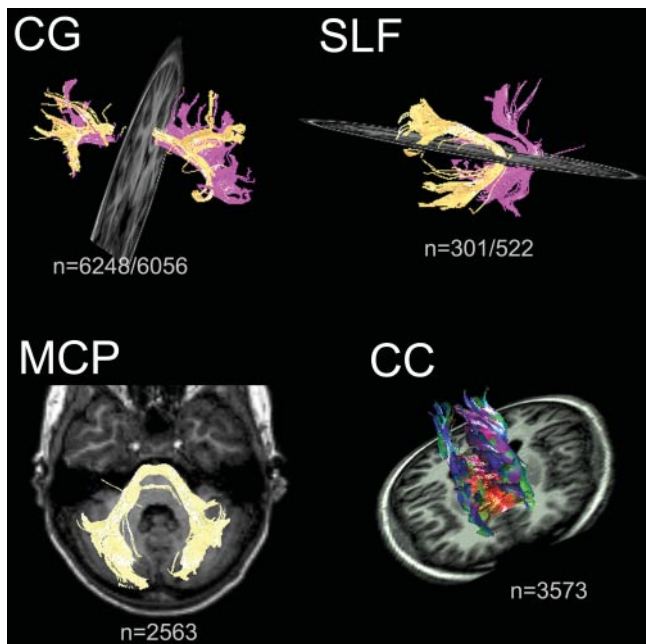

Fig. 8 Cingulate fasciculus (CG), superior longitudinal fasciculus (SLF), middle cerebellar peduncle (MCP) and the corpus callosum (CC). There were no statistically significant changes noted in CG (shown P3), SLF (P4) and MCP (P2) in patients. The CC showed a reduction in number of fibres in the patient (P1). *n* = DTI fibre count.

more fibres were noted on the left side compared with the right side.

ROI analysis

The results of the ROI analysis are summarized in Table 4 and in Fig. 9.

Changes on the affected side of the PWI patients

At the site of primary periventricular insult, there was statistically significant reduction in FA ($P = 0.0007$) and marked elevation in D_{av} ($P = 0.0007$) in the patient group compared with the control group. There was a significant reduction in FA in CST measured in the medulla and lower pons on the affected side of the patients ($P = 0.0400$, and 0.0127,

respectively). Finally, there was a significant reduction in FA in the body of the CC ($P = 0.0079$).

Among the deep grey matter regions studied, the thalamus showed similar findings as the primary site of insult, i.e. a marked reduction in FA ($P = 0.0027$) and significant elevation in D_{av} ($P = 0.0280$). The head of caudate and the lentiform nucleus showed marked reduction in FA ($P = 0.0193$ and 0.0280, respectively) and no significant change in $D_{av.}$

Changes on the unaffected side of the PWI patients

In the ROI symmetrically positioned opposite the lesion in the normal appearing white matter in the unaffected hemisphere of the patients, there was a significant reduction in D_{av} ($P = 0.0013$) as compared with controls. Within the CST, there was a significant reduction in D_{av} in the medulla ($P = 0.0280$) and nearly significant in the upper pons ($P = 0.0992$). More importantly, there was a significant increase in mean FA value on the unaffected side of patients compared with controls in the CST at the level of the medulla ($P = 0.0027$) and upper pons ($P = 0.0007$).

Finally also a significant reduction in FA value of the caudate was noted ($P = 0.0047$).

Cross-sectional area ratio measurements on pyramidal tracts in upper pons

There was a significant reduction in the ratio of cross sectional area of CST on the affected side to total cross-sectional area of upper pons, compared with control subjects on both the sides ($2.55 \pm 0.54\%$ versus $8.18 \pm 3.00\%$, $P = 0.0020$). There was also a significant reduction in this ratio on the affected side of the patients compared with the unaffected side ($P = 0.0286$). No difference was noted between the unaffected side of patients and the controls or between either side of the controls (See also Fig. 2B and Table 5).

Discussion

DTI has been applied for studying disorders of the brain for about a decade, and allows the measurements of both

Table 4. Region of interest analysis of diffusion parameters in controls and patients

Regions	FA				D_{av}				P-value FA		P-value D_{av}		Lesion type inference	Contralateral type inference
	CL R	CL L	PT Aff	PT Unaff	CL R	CL L	PT Aff	PT Unaff	PT Aff versus CL	PT Unaff versus CL	PT Aff versus CL	PT Unaff versus CL		
Primary site	0.53	0.54	0.34	0.53	0.83	0.81	1.30	0.68	**0.0007**	0.5941	**0.0007**	**0.0013**	FA↓, D_{av}↑ primary lesion	FA =, D_{av}↓ compaction?
CST Medulla	0.47	0.47	0.38	0.60	1.29	1.33	1.31	0.92	**0.0400**	**0.0027**	1.0000	**0.0280**	FA↓, D_{av} = Wallerian degeneration	FA↑, D_{av}↓ compaction?
CST Low Pons	0.49	0.50	0.39	0.52	0.78	0.76	0.80	0.81	**0.0127**	0.4396	0.1292	0.2065	FA↓, D_{av} = Wallerian degeneration	–
CST Upp Pons	0.51	0.54	0.50	0.59	0.75	0.76	0.77	0.73	0.5941	**0.0007**	0.4396	0.0992	–	FA↑, D_{av}↓ compaction?
Thalamus	0.31	0.32	0.28	0.30	0.77	0.77	0.80	0.77	**0.0027**	0.3097	**0.0280**	0.2222	FA↓, D_{av}↑ primary lesion	–
Caudate nucleus	0.28	0.25	0.21	0.22	0.81	0.82	0.79	0.76	**0.0193**	**0.0047**	0.5941	**0.0280**	FA↓, D_{av} = secondary degeneration	FA↓, D_{av}↓
Lentiform nucleus	0.22	0.24	0.20	0.22	0.76	0.75	0.74	0.75	**0.0280**	0.7679	0.5941	0.4396	FA↓, D_{av} = secondary degeneration	–
CC- Genu rostrum	0.66		0.65		0.93		0.93		0.8413		0.6905		–	–
CC- Body	0.57		0.41		0.85		1.29		**0.0079**		0.1508		FA↓, D_{av} = secondary degeneration	–
CC- Splenium	0.72		0.71		0.95		0.93		1.0000		1.0000		–	–

Mann–Whitney U test was used for all comparisons, the statistical significance level was set at $P = 0.05$. Significant ones are marked in bold. R, right; L, left; PT, patients; CL, controls; Aff, affected side; Unaff, unaffected side; Low, lower; Upp, upper; CST, corticospinal tract; CC, corpus callosum; FA, fractional anisotropy; D_{av}, directionally averaged mean diffusivity (Trace D/3).
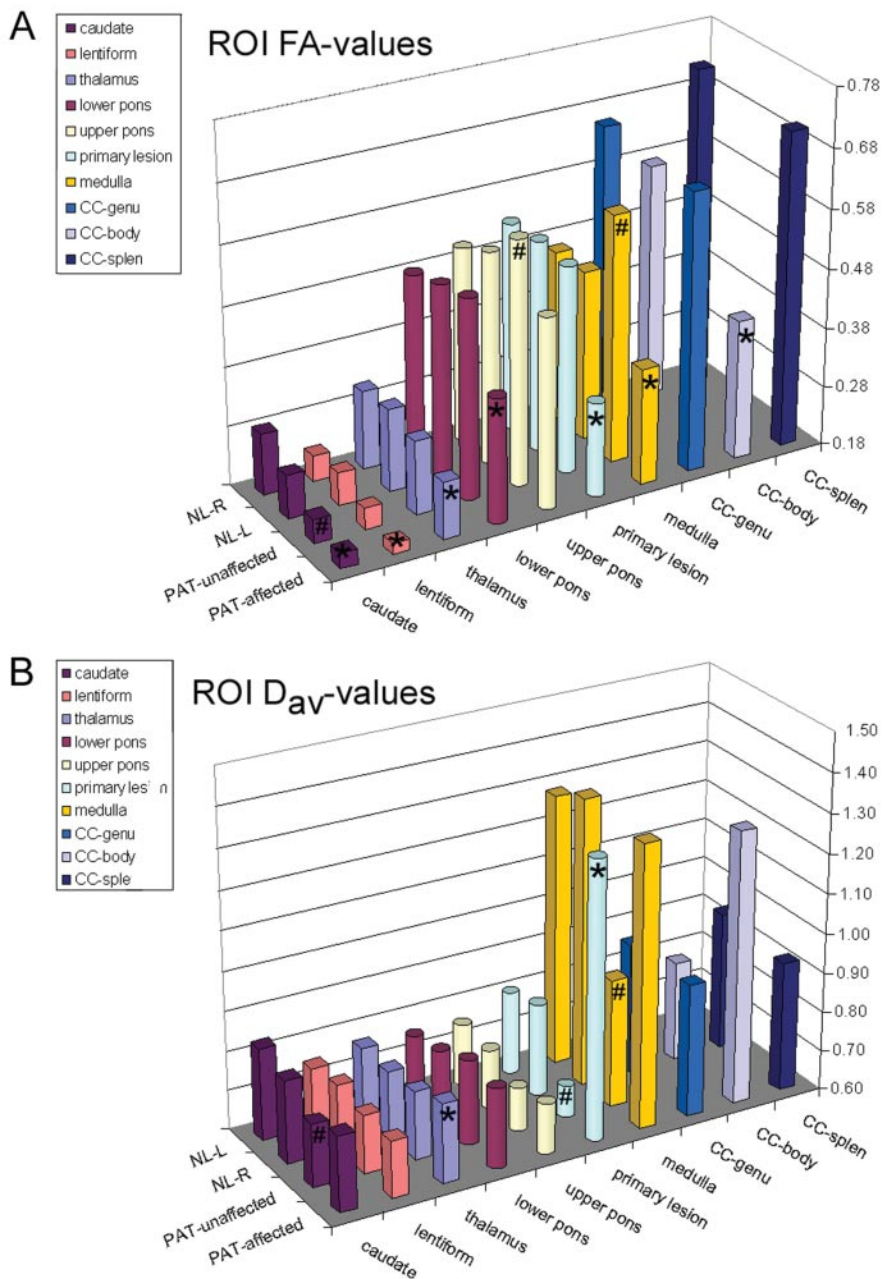
Fig. 9 ROI analysis. The results of the ROI analysis of diffusion parameters at the primary site of white matter injury, in various deep grey matter nuclei, CST in the brain stem at various levels and the CC are shown. Note the reduction in FA (**A**) and the increase in Dav (**B**) corresponding to primary and secondary degenerations at various sites on the affected side in patients (see also Table 4, and the text). There is also a 'compensatory' increase in FA and a reduction in Dav in CST at various levels in the brainstem, suggesting the reorganization of this tract on the unaffected side in spastic hemiparetics. (* = statistically significant change on the affected side of patients and # = same on the unaffected side of patients).

magnitude and direction of *in vivo* water diffusion (Pierpaoli and Basser, 1996; Pierpaoli *et al.*, 1996). Within the packed white matter structural organization, the movement of water molecules is maximal parallel to the axonal axes (Le Bihan *et al.*, 1986; Moseley *et al.*, 1990; Pierpaoli *et al.*, 1996). While myelin plays an important role in determining this anisotropy of white matter, it is not the only factor responsible. Various studies have shown that the axonal membrane, the

Table 5 Ratio of cross sectional area of the pyramidal tract and the upper pons

Ratio	Controls (Right) (%)	Controls (Left) (%)	PT unaffected (%)	PT affected (%)
Mean	8.29	8.07	7.86	2.55
SD	3.09	2.91	1.75	0.54

SD, standard deviation; PT, patients.

number and thickness of axons, tissue hydration, cell packing density and intravoxel directional coherence of the fibres influence this directional component of diffusion (Shimony et al., 1999; Virta et al., 1999; Barkovich, 2000). Although the global diffusion parameters reach normal adult levels by around 5 to 6 years of age, some association tracts continue to show changes in diffusion properties throughout adolescence, suggesting the occurence of microstructural organizational 'fine tuning' in these tracts (Shimony et al., 1999; Mukherjee et al., 2001; Schmithorst et al., 2002). We selected the present age group of patients to minimize the bias due to age related changes on diffusion parameters and to avoid the need for sedation or general anaesthesia for MR examination.

PWI is a major form of brain injury in spastic hemiplegia (Niemann, 2000). Contrary to patients with spastic diplegia and PWI, many hemiplegics with PWI are born at term. Nevertheless, it is assumed that the pathogenesis for both groups is similar, and consists of an insult to the developing brain at the early third trimester of gestation (Niemann, 2000). In patient 3 of this study, an insult at the corresponding time-frame has been documented; for the other patients the causal insult was less clear or remained clinically silent. In patients with PWI, other regions of the brain like the deep grey matter nuclei and various neuronal pathways including the pyramidal tract were also shown to be involved (Yokochi et al., 1997; Staudt et al., 2000, 2003; Lin et al., 2001; Glenn et al., 2003). The secondary Wallerian degeneration of the CST has been the subject of many recent research papers (Staudt et al., 2000; Pierpaoli et al., 2001; Glenn et al., 2003). Pierpaoli et al. (2001) have shown that the diffusion tensor parameters significantly differ in primary and secondary degeneration of human white matter. Others studied the role of sensory pathways in the motor outcome of these children (Hoon et al., 2002; Lee et al., 2005).

The present study was divided into two major parts,

(i) Analysis of various fibre tracts of the brain, which are likely to be involved in such a lesion.
(ii) ROI-based analysis of the primary lesion site, the deep grey matter, the CC and the pyramidal tract at different levels in the brainstem.

The fibre tracts

This study has shown that there is a statistically significant reduction in DTI fibre count along the CST and CBT on the side ipsilateral to the periventricular lesion compared with control subjects. While this was in conjunction with other studies showing degeneration of CST, the involvement of CBT by these lesions is emphasized in the present study. However, some of the previous studies might have included this tract also in the estimation of CST, owing to ambiguous definition of descending tracts and/or partial volume effects (Virta et al., 1999; Staudt et al., 2000; Pierpaoli

et al., 2001). There has been a reduction in anisotropy and an increase in mean diffusivity noted along these tracts, largely by the contribution of the primary sites of brain degeneration.

More interestingly, there was an absolute increase in DTI fibre count noted on the contralateral side of the lesion in all the spastic hemiparesis patients compared with controls, though it reached the level of statistical significance only in the case of CBT. These DTI fibre tract parameter changes may not necessarily translate into an absolute increase in the number of axons, as it is too early to draw microscopic inferences from a diffusion change observed in a macroscopic domain, especially with the current resolution of DTI sequences. However, this definitely means that there is a microstructural reorganization happening in these fibre tracts on the unaffected side. This may be a compensatory mechanism developing in these children, who are affected by a brain injury in a very early stage of development. This observation is not shared (or not considered) by other similar studies using DTI (Glenn et al., 2003). Several authors have noted compensatory hypertrophy of the contralateral pyramidal tract (CST) in autopsy studies in adults who had possible congenital hemiparesis (Déjérine and Déjérine, 1902; Verhaar, 1950; Scales and Collins, 1972; Schachenmayr and Friede, 1978). They also found an increase in the number of fibres in the unaffected CST in these patients compared with the control subjects. This issue is further addressed when we discuss the ROI analysis.

Recently there have been a few MR demonstrations of possible involvement of the sensory pathways in the pathogenesis of motor deficit and spasticity in PWI. (Yokochi et al., 1997; Hoon et al., 2002; Lee et al., 2005). Hoon et al. have suggested the possible contribution of PTR in the motor outcome of patients with bilateral PWI (Hoon et al., 2002). Besides the widely accepted concept of involvement of CST in this condition, they showed in two bilaterally involved patients that the motor impairment in PWI may reflect disruption of sensory connections. The present study showed significant involvement (reduction in DTI fibre count) of the ipsilateral superior thalamic radiation and no change in the ATR or PTR in hemiplegic patients. This emphasizes the involvement of the STR in such patients. The unilateral involvement of the STR (and not the ATR or PTR) can be readily explained by the direct connection of the STR, originating in the ventral nuclei of the thalamus, to the postcentral gyrus, from where connection to the damaged corticobulbar and corticospinal pathways is obvious. The fibres of PTR showed a more complex distribution of changes, both in controls and in patients. There were significantly more fibres detected on the left side of control subjects in the case of PTR. While we noted this trend of more fibres being generated on the left side in the CST in controls, it also failed to reach statistical significance. One can assume that the asymmetry is related to handedness or language lateralization, but further investigation with a larger control group is required before commenting on the significance of this finding.

These findings suggest that both sensory and motor pathways are affected to various extents in patients with PWI and a complex interplay of relative involvement of these pathways might define the final clinical outcome of these patients, and not the degeneration of either of them alone, as hinted by previous studies (Staudt *et al.*, 2000, 2003; Hoon *et al.*, 2002; Glenn *et al.*, 2003). In addition, the role of involvement of deep grey matter nuclei also needs to be addressed (discussed below).

Interestingly, the CC, CG, SLF and the MCP showed no significant degenerative changes by DTI parameters. These fascicles were selected to be included in the study because of their anatomical proximity to those tracts, and their involvement in PWI either primarily or secondarily has already been proved.

The CC in our patient group showed fewer fibres as compared with controls but without statistical significance. Hoon *et al.* (2002) found a severe reduction in size of the posterior CC, and it is well known that in cerebral palsy, thinning of the CC is often found (Davatzikos *et al.*, 2003). We speculate that the mild involvement of our patients, or the fact that they all showed a unilateral motor impairment, explain our findings; but this remains to be proven.

Hoon *et al.* had also observed non-involvement of CG and SLF in PWI. This could prove that antegrade or retrograde secondary axonal degeneration is not happening in these pathways because they are not functionally connected to the primary sites of insult in PWI. However, this assumption may not be entirely true, as we know that the middle cerebellar peduncle carries information involved in the processing of complex motor tasks, between the cerebellum and the pons. A more intricate mechanism of secondary tract degeneration in complex motor pathways with a probable role for synaptic connections within it may be implicated.

ROI measurements

ROI analysis gave remarkably supportive evidence for the observations made on fibre tract studies. Fractional anisotropy and mean diffusivity measured on long tracts are generally averaged values along the entire length of these tracts. Precise ROI measurements made on orientation colour maps represent changes occurring in a particular location in a pathway with a focal perspective which is more relevant as these values also depend on the intravoxel directional coherence of tracts in a particular brain region (Virta *et al.*, 1999; Pierpaoli *et al.*, 2001). The primary site of periventricular insult showed a marked reduction in FA and a significant increase in D_{av}. This is in agreement with the previously described 'DTI signature' of primary white matter insult (Pierpaoli *et al.*, 2001). This can be explained by the marked gliosis and microscopic or macroscopic cystic changes occurring at the site of a primary lesion.

More interestingly, there was a significant reduction in mean diffusivity in the contralateral periventricular white matter compared with controls, measured on carefully and symmetrically placed ROI in the five spastic hemiparesis patients. We know that even in hemiparetic patients with PWI there can be bilateral brain lesions, which are not detected on conventional MRI. However, we expected an increase in mean diffusivity on the unaffected side, but actually there was a decrease. This may point more towards reorganization of the contralateral white matter rather than subclinical insult by PWI.

The regional analysis of CST in the brainstem added further insight to the understanding of the pathogenesis of degeneration taking place on the side of the lesion and a possible 'compensatory' reorganization occurring on the contralateral side. The affected side showed the 'DTI signature' of Wallerian degeneration (marked decrease in anisotropy without increase in diffusivity) (Pierpaoli *et al.*, 2001). The reason for this deviation from the changes occurring in primary lesions is that very little microcystic water accumulation occurs at the site of secondary degeneration. Pierpaoli and Barnett have shown that the regional diffusion changes occurring in Wallerian degeneration differ in different parts of the brainstem and are largely determined by the directional coherence of fibres in that region (Pierpaoli *et al.*, 2001). They observed only a mild decrease in FA in the upper pons at the side of Wallerian degeneration, as compared with a marked decrease in other brainstem regions and we could confirm this observation.

A more interesting finding, which was in agreement with the results of the fibre tract statistics, was the observed change in diffusion parameters in the 'unaffected' pyramidal tract in the patients. There was an increase in anisotropy of this tract in the brainstem, which reached significant levels in medulla and upper pons. Also there was a significant reduction in mean diffusivity noted in the medulla. These changes may suggest the possible reorganization of this tract, which may mean an increase in the 'compactness' (see Table 4) by which these fibres are arranged along with probable alterations in the microstructure of the cellular matrix surrounding them. An associated alteration in myelination pattern of these fibres can also not be entirely ruled out. Also, the complex process of activity-dependent 'pruning' that normally takes places during the first years of life throughout adolescence, might have had a role in the development of the different properties of the 'unaffected' CBT and CST observed in our patients. The diminished motor experience secondary to the motor handicap at the affected side, might have influenced the process of reorganization that normally, driven by stimulation from the external environment and primary senses, eliminates the excess of neurons and synaptic connections produced during prenatal and early postnatal development (Johnston *et al.*, 2001*b*). This might have contributed to an enlarged CBT and more 'compact' CST in the unaffected hemisphere. This reorganization was not reported before in studies involving focal infarcts in adults and may be a unique process occurring exclusively in the young brains (Wieshmann *et al.*, 1999; Pierpaoli *et al.*, 2001). Staudt *et al.* recently (2005) in a group

of congenital hemiplegics reported focal areas of hyper-intensity at the level of the pons on routine T2-weighted magnetic resonance imaging, in the course of the CST of the contralesional hemisphere. Because they found these hyperintensities in a total of 6 out of 10 patients who showed evidence of ipsilateral corticospinal projections as validated by transcranial magnetic stimulation, they speculated that this might point to reorganization of the contralesional corticospinal pathways. As previously mentioned, several autopsy studies have addressed this issue. Scales and Collins (1972) and Schachenmayr and Friede (1978) have demonstrated an absolute increase in number, thickness and a change in the myelination pattern of these fibres in the unaffected tracts in congenital hemiparetics. The latter authors have demonstrated dystopic myelination with myelin sheaths that contained glial cell bodies, presumably oligodendroglia, instead of axons in these tracts. They also noted a lack of increase in the number of Betz cells in the corresponding sensory motor cortex in such patients. So they proposed that these changes in the CST might be a possible compensatory mechanism by increased connectivity of the uncrossed fibres to the hemiparetic side of the patient. More recently Uematsu et al. could reproduce these effects by experimental studies on newborn mice with induced unilateral motor cortical damage by cryocoagulation (Uematsu et al., 1996). They also demonstrated a functional recovery in them later (on post-procedure day 10). Our results also point to these conclusions, but how far this acts as a functional compensatory mechanism needs to be addressed further with transcranial magnetic cortical stimulation and/or fMRI experiments.

Although the CC showed no significant decrease in fibre count in patients compared with controls, changes in diffusion (reduced FA without increased D_{av}) were found in the body region. The fibres connecting the motor cortices, which mediate interhemispheric inhibitory signals of motor activity, pass through the mid and posterior body of CC (Davatzikos et al., 2003). By callosal morphometry, using the method of shape transformations, Davatzikos et al. have shown that in PWI patients with motor deficits especially the body of the CC was atrophied (Davatzikos et al., 2003). Our findings confirm this observation, making use of diffusion parameters, which are theoretically much more sensitive in evaluating this correlation than the changes in shape of the CC.

The deep grey matter nuclei also showed diffusion changes. On the affected side, the thalamus showed significant reduction in FA and increase in D_{av}. In the other two nuclei FA reduction was the only significant finding. If the experience obtained from white matter pathways can be directly extrapolated onto these grey matter formations, the thalamus is showing features suggestive of primary involvement by the insult and the other two nuclei of secondary degeneration. Various authors have noted involvement of the deep grey matter nuclei in PWI using conventional MRI techniques (Yokochi et al., 1997; Lin et al., 2001). However, the exact

pathogenesis of this involvement remained unexplained. DTI may throw a new light into this area.

Further evidence on Wallerian degeneration of CST in the brainstem

Staudt et al. found a good correlation between motor impairment in congenital hemiplegics and the lateral extent of the periventricular lesion, measured on semi-coronal planes along the course of the CST from the precentral gyrus to the internal capsule on conventional MR images (Staudt et al., 2000). They also showed that asymmetry ratio measurements in the brainstem on axial anatomic images could predict the degree of Wallerian degeneration of the pyramidal tract in PWI (Staudt et al., 2000). However, this method was plagued by the dependence on expected gross asymmetric deformations of brainstem caused by degeneration of a tract that occupies normally only <10% of the total cross-sectional area. As expected they could use it only in severe cases of Wallerian degeneration, and they obtained good correlation with motor disability only for measurements in the medulla. Obviously this technique cannot be used in bilateral degeneration of the CST. Our method of determining actual ratio measurements of cross-sectional area of CST and of brainstem on DTI colour maps and coregistered anatomy scans eliminates most of these biases. However, it should be noted that a ratio of the cross-sectional area of the CST to brainstem is not free of bias, since the denominator of the ratio (brainstem area) is affected by the area of the CST as well. We selected upper pons as the site of choice, because it was observed to be the most difficult region to detect brainstem asymmetry on anatomic scans (Staudt et al., 2000). Nevertheless, this area ratio measurement proved to be a useful indicator of the severity of Wallerian degeneration and was in agreement with the findings of CST fibre statistics on the affected side as discussed earlier. This may prove to be a quick and useful parameter to assess lesion severity in PWI in clinical DTI imaging.

Limitations of the study

The study was limited by the relatively small number of subjects included, and the low statistical power of the non-parametric test used for the analysis. The variability in DTI fibre count, FA and D_{av} values was larger in the patients (as opposed to the controls) and is probably due to different lesion size. Also, we set different anisotropy and inner product thresholds for generating different fibre bundles. But this was necessary to obtain good fibre tracts without 'contamination' from adjacent ones, especially because we were not using a 'NOT' operator to deliberately eliminate some generated fibres as proposed by other authors (Wakana et al., 2004). Since we used the same parameters for all the subjects, in a particular fibre bundle, inter group comparison for that bundle was still possible, while comparison between different tracts was not feasible, and was not our aim. We also

agree that all the limitations of current DTI techniques, such as limited spatial resolution, intravoxel averaging of anisotropy by adjacent tracts, partial volume effects and image artefacts might have affected the results, but equally in both patient and control groups. Also, no attempt was made to study the correlation of somatotopic distribution of diffusion parameter changes in the brain with motor dysfunctions of hand and leg in patients. In our opinion, fMRI guided DTI and/or transcranial magnetic cortical stimulation will be essential to gaining any meaningful evaluation of this aspect of motor function.

Conclusions

DTI has given a new insight into the pathophysiological mechanism leading to changes occurring in both white matter and deep grey matter in PWI. The diffusion tensor 'signature' may be of use in differentiating between the primary site of involvement and the secondary degeneration in this condition. A complex interplay of degree of degeneration of various motor, sensory and possibly commissural pathways, as well as the involvement of deep grey matter nuclei in the brain may be defining the final clinical outcome in these patients. There is evidence for reorganization towards more compaction of the pyramidal tract in the brainstem on the unaffected side in patients with spastic hemiparesis and unilateral PWI. In addition, there is a significant increase in the DTI fibre count in the CBT of the unaffected hemisphere of PWI patients. How far this acts as a functional compensatory mechanism needs to be validated with future fMRI and transcranial magnetic cortical stimulation studies.

Acknowledgements

References

Banker LL, Larroche JC. Periventricular leukomalacia of infancy. Arch Neurol 1962; 7: 386–410.

Barkovich AJ. Concepts of myelin and myelination in neuroradiology. AJNR Am J Neuroradiol 2000; 21: 1099–109.

Basser PJ, Pierpaoli C. Microstructural and physiological features of tissues elucidated by quantitative-diffusion-tensor MRI. J Magn Reson 1996; 111: 209–19.

Basser PJ, Pierpaoli C. A simplified method to measure the diffusion tensor from seven MR images. Magn Reson Med 1998; 39: 928–34.

Basser PJ, Pajevic S, Pierpaoli C, Duda J, Aldroubi A. In vivo fiber tractography using DT-MRI data. Magn Reson Med 2000; 44: 625–32.

Cioni G, Bartalena L, Biagioni E, Boldrini A, Canapicchi R. Neuroimaging and functional outcome of neonatal leukomalacia. Behav Brain Res 1992; 49: 7–19.

Davatzikos C, Barzi A, Lawrie T, Hoon H, Melhem R. Correlation of corpus callosal morphometry with cognitive and motor function in periventricular leukomalacia. Neuropediatrics 2003; 34: 247–52.

Déjérine J, Déjérine A. Sur l'hypertrophie compensatrice du faisceau pyramidal du côté sain, dans un cas d'hémiplégie cérébrale infantile. Rev Neurol 1902; 10: 642–6.

de Vries LS, Roelants-Van Rijn AM, Rademaker KJ, Van Haastert IC, Beek FJ, Groenendaal F. Unilateral parenchymal haemorrhagic infarction in the preterm infant. Eur J Paediatr Neurol 2001; 5: 139–49.

Glenn OA, Henry RG, Berman JI, Chang PC, Miller SP, Vigneron DB, et al. DTI-based three-dimensional tractography detects differences in the pyramidal tracts of infants and children with congenital hemiparesis. J Magn Reson Imaging 2003; 18: 641–8.

Hagberg B, Hagberg G, Beckung E, Uvebrant P. Changing panorama of cerebral palsy in Sweden. VIII. Prevalence and origin in the birth year period 1991–94. Acta Pediatr 2001; 90: 271–7.

Hashimoto K, Hasegawa H, Kida Y, Takeuchi Y. Correlation between neuroimaging and neurological outcome in periventricular leukomalacia: diagnostic criteria. Pediatr Int 2001; 43: 240–5.

Hoon AH Jr, Lawrie WT Jr, Melhem ER, Reinhardt EM, van Zijl PC, Solaiyappan BE, et al. Diffusion tensor imaging of periventricular leukomalacia shows affected sensory cortex white matter pathways. Neurology 2002; 59: 752–6.

Johnston MV, Trescher WH, Ishida A, Nakajima W. Neurobiology of hypoxic-ischemic injury in the developing brain. Pediatr Res 2001a; 49: 735–41.

Johnston MV, Nishimura A, Harum K, Pekar J, Blue ME. Sculpting the developing Brain. Adv Pediatr 2001b; 48: 1–38.

Kwong KL, Wong YC, Fong CM, Wong SN, So KT. Magnetic resonance imaging in 122 children with spastic cerebral palsy. Pediatr Neurol 2004; 31: 172–6.

Le Bihan D, Basser PJ. Molecular diffusion and nuclear magnetic resonance. Le Bihan D, editor. New York: Raven Press; 1995. p. 5–7.

Le Bihan D, Breton E, Lallemand D, Grenier P, Cabanis E, Laval-Jeantet M. MR imaging of intravoxel incoherent motions: application to diffusion and perfusion in neurologic disorders. Radiology 1986; 161: 401–7.

Lee SK, Kim DI, Kim J, Kim DJ, Kim HD, Kim DS, et al. Diffusion-tensor MR imaging and fiber tractography: a new method of describing aberrant fiber connections in developmental CNS anomalies. Radiographics 2005; 25: 53–65; discussion 66–8.

Lin Y, Okumura A, Hayakawa F, Kato K, Kuno T, Watanabe K. Quantitative evaluation of thalami and basal ganglia in infants with periventricular leukomalacia. Dev Med Child Neurol 2001; 43: 481–5.

Makris N, Worth AJ, Sorensen AG, Papadimitriou GM, Wu O, Reese TG, et al. Morphometry of in vivo human white matter association pathways with diffusion weighted magnetic resonance imaging. Ann Neurol 1997; 42: 951–62.

Marti-Bonmati L, Rodrigo C, Torregrosa A, Menor F, Dosda R, Poyatos C. The relation between the clinical symptoms and the findings on magnetic resonance in children with periventricular leukomalacia. Rev Neurol 2001; 33: 22–6.

Melhem ER, Hoon AH Jr, Ferrucci JT Jr, Quinn CB, Reinhardt EM, Demetrides SW, et al. Periventricular leukomalacia: relationship between lateral ventricular volume on brain MR images and severity of cognitive and motor impairment. Radiology 2000; 214: 199–204.

Mori S, Crain BJ, Chacko VP, van Zijl PC. Three-dimensional tracking of axonal projections in the brain by magnetic resonance imaging. Ann Neurol 1999; 45: 265–9.

Mori S, Kaufmann WE, Davatzikos C, Stieltjes B, Amodei L, Fredericksen K, et al. Imaging cortical association tracts in human brain. Magn Reson Med 2002; 47: 215–23.

Moseley ME, Cohen Y, Kucharczyk J, Mintorovitch J, Asgari HS, Wendland MF et al. Diffusion-weighted MR imaging of anisotropic water diffusion in cat central nervous system. Radiology 1990; 176: 439–45.

Mukherjee P, Miller JH, Shimony JS, Conturo TE, Lee BC, Almli CR, et al. Normal brain maturation during childhood: developmental trends characterized with diffusion-tensor MR imaging. Radiology 2001; 221: 349–58.

Niemann G. A new MRI-based classification. In: Neville B, Goodman R, editors. Congenital hemiplegia. Clinics in Developmental Medicine. London: Mac Keith Press; 2000. p. 37–52.

Pajevic S, Pierpaoli C. Color schemes to represent the orientation of anisotropic tissues from diffusion tensor data: application to white matter fiber tract mapping in the human brain. Magn Reson Med 1999; 42: 526–40.

Palisano R, Rosenbaum P, Walter S, Russell D, Wood E, Galuppi B. Development and reliability of a system to classify gross motor function in children with cerebral palsy. Dev Med Child Neurol 1997; 39: 214–23.

Payam R, Andrew D. Periventricular leukomalacia, inflammation and white matter lesions within the developing nervous system. Neuropathology 2002; 22: 106–32.

Pierpaoli C, Basser JP. Toward a quantitative assessment of diffusion anisotropy. Magn Reson Med 1996; 36: 893–906.

Pierpaoli C, Jezzard P, Basser PJ, Barnett A, Di Chiro G. Diffusion tensor MR imaging of the human brain. Radiology 1996; 201: 637–48.

Pierpaoli C, Barnett A, Pajevic S, Chen R, Penix LR, Virta A, et al. Water diffusion changes in Wallerian degeneration and their dependence on white matter architecture. Neuroimage 2001; 13: 1174–85.

Scales DA, Collins GH. Cerebral degeneration with hypertrophy of the contralateral pyramid. Arch Neurol 1972; 26: 186–90.

Schachenmayr W, Friede RL. Dystopic myelination with hypertrophy of pyramidal tract. J Neuropathol Exp Neurol 1978; 37: 34–44.

Schmithorst VJ, Wilke M, Dardzinski BJ, Holland SK. Correlation of white matter diffusivity and anisotropy with age during childhood and adolescence: a cross-sectional diffusion-tensor MR imaging study. Radiology 2002; 222: 212–8.

Schouman-Claeys E, Henry-Feugeas MC, Roset F, Larroche JC, Hassine D, Sadik JC, et al. Periventricular leukomalacia: correlation between MR imaging and autopsy findings during the first 2 months of life. Radiology 1993; 189: 59–64.

Shimony JS, McKinstry RC, Akbudak E, Aronovitz JA, Snyder AZ, Lori NF, et al. Quantitative diffusion-tensor anisotropy brain MR imaging: normative human data and anatomic analysis. Radiology 1999; 212: 770–84.

Staudt M, Niemann G, Grodd W, Krägeloh-Mann I. The pyramidal tract in congenital hemiparesis: relationship between morphology and function in periventricular lesions. Neuropediatrics 2000; 31: 257–64.

Staudt M, Pavlova M, Böhm S, Grodd W, Krägeloh-Mann I. Pyramidal tract damage correlates with motor dysfunction in bilateral periventricular leukomalacia (PVL). Neuropediatrics 2003; 34: 182–8.

Staudt M, Krageloh-Mann I, Grodd W. Ipsilateral corticospinal pathways in congenital hemiparesis on routine magnetic resonance imaging. Pediatr Neurol 2005; 32: 37–9.

Takanashi J, Barkovich AJ, Ferriero DM, Suzuki H, Kohno Y. Widening spectrum of congenital hemiplegia: periventricular venous infarction in term neonates. Neurology 2003; 61: 531–3.

Uematsu J, Ono K, Yamano T, Shimada M. Development of corticospinal tract fibers and their plasticity. II. Neonatal unilateral cortical damage and subsequent development of the corticospinal tract in mice. Brain Dev 1996; 18: 173–8.

Verhaart W. Hypertrophy of peduncle and pyramid as a result of degeneration of contralateral corticofugal fiber tracts. J Comp Neurol 1950; 92: 1–15.

Virta A, Barnett A, Pierpaoli C. Visualizing and characterizing white matter fiber structure and architecture in the human pyramidal tract using diffusion tensor MRI. Magn Reson Imaging 1999; 17: 1121–33.

Volpe JJ. Neurobiology of periventricular leukomalacia in the premature infant. Pediatr Res 2001; 50: 553–62.

Wakana S, Jiang H, Nagae-Poetscher LM, van Zijl PC, Mori S. Fiber tract-based atlas of human white matter anatomy. Radiology 2004; 230: 77–87.

Wieshmann UC, Clark CA, Symms MR, Franconi F, Barker GJ, Shorvon SD. Anisotropy of water diffusion in corona radiata and cerebral peduncle in patients with hemiparesis. Neuroimage 1999; 10: 225–30.

Yokochi K. Thalamic lesion revealed by MR associated with periventricular leukomalacia and clinical profiles of subjects. Acta Paediatr 1997; 86: 493–6.